

Fluorogenic Probe for Constitutive Cellular Endocytosis

Michael N. Levine,¹ Trish T. Hoang,¹ and Ronald T. Raines^{1,2,*}

¹Department of Biochemistry, University of Wisconsin–Madison, 433 Babcock Drive, Madison, WI 53706, USA

²Department of Chemistry, University of Wisconsin–Madison, 1101 University Avenue, Madison, WI 53706, USA

*Correspondence: rtraines@wisc.edu

<http://dx.doi.org/10.1016/j.chembiol.2013.03.016>

SUMMARY

Endocytosis is a fundamental process of eukaryotic cells that is critical for nutrient uptake, signal transduction, and growth. We have developed a molecular probe to quantify endocytosis. The probe is a lipid conjugated to a fluorophore that is masked with an enzyme-activatable moiety known as the trimethyl lock. The probe is not fluorescent when incorporated into the plasma membrane of human cells but becomes fluorescent upon internalization into endosomes, where cellular esterases activate the trimethyl lock. Using this probe, we found that human breast cancer cells undergo constitutive endocytosis more rapidly than do matched noncancerous cells. These data reveal a possible phenotypic distinction of cancer cells that could be the basis for chemotherapeutic intervention.

INTRODUCTION

Endocytosis is the key regulator of macromolecular internalization into eukaryotic cells (Conner and Schmid, 2003). In this intricate process, proteins mediate the invagination of the plasma membrane and then its fusion to pinch off a lipid-bilayer-encased vesicle within a cell (Doherty and McMahon, 2009). Many endocytic pathways operate in parallel. The most-studied pathway, clathrin-mediated endocytosis, occurs constitutively in all cell types and generally involves the binding of a ligand to a receptor prior to internalization (McMahon and Boucrot, 2011). Another pathway, caveolae-mediated endocytosis, is characterized by vesicles enriched in glycosphingolipids, cholesterol, and the integral membrane protein caveolin (Hansen and Nichols, 2009). These endocytic pathways are the portals for delivery of essential nutrients, such as iron via transferrin and cholesterol via lipoprotein particles. Deleteriously, these pathways can facilitate the transit of pathogens (Gruenberg and van der Goot, 2006; Kerr and Teasdale, 2009).

Endocytosis regulates the concentration of cell-surface receptors by transporting them to and from the plasma membrane (Mosesson et al., 2008). Accordingly, endocytosis has a direct influence on signal transduction pathways that can malfunction in cancer patients (Hanahan and Weinberg, 2011). Conversely, differences in endocytosis between cancerous and noncancerous cells could lead to new treatment options.

For example, pancreatic-type ribonucleases (ptRNases) have emerged as putative cancer chemotherapeutic agents (Lee and Raines, 2008; Arnold, 2008; Fang and Ng, 2011; Lomax et al., 2012). These cationic enzymes are internalized by receptor-independent endocytosis and then escape from endosomes to the cytosol, where they catalyze the degradation of cellular RNA. The basis for their cancer-cell-specific toxicity is not clear, but could entail differential rates of endocytosis.

Two types of assays have been used to monitor constitutive endocytosis (Ivanov, 2007). In one, endocytosis has been quantified by assaying the uptake of soluble enzymes, such as horseradish peroxidase (Steinman and Cohn, 1972). Data are acquired by fixing cells and then staining them with a colorimetric substrate. This assay is discontinuous and vulnerable to the artifacts that can accompany the use of fixed cells (Richard et al., 2003). Alternatively, the fate of a fluorescent lipid has been monitored continuously by microscopy (Kok et al., 1990; Cochilla et al., 1999; Maier et al., 2002; Rea et al., 2004; Bissig et al., 2012). These assays require extensive washing to remove unincorporated lipid and are not amenable to automated cell counting and sorting techniques.

We sought to develop a facile means to assess endocytosis continuously in live cells. An ideal molecular probe would have no background fluorescence and would be able to distinguish the lumen of endosomes from the plasma membrane. We reasoned that a lipid with a head group that is responsive to an endosomal enzyme could serve as the basis as such a probe, as fluorescence generated over time would reflect the rate of endocytosis. Here, we report on the efficacy of our strategy.

RESULTS AND DISCUSSION

To test our strategy, we designed lipid **1**. Lipid **1** contains a “trimethyl lock” moiety in which an acetyl ester acts as a molecular trigger (Levine and Raines, 2012). This ester linkage is known to be stable to hydrolysis at physiological pH (Chandran et al., 2005; Lavis et al., 2006a, 2006b; Levine et al., 2008). Although the ester linkage in lipid **1** is insulated from the fluorophore, its hydrolysis is coupled to the cleavage of its otherwise recalcitrant amide bond. Analogous probes have been used to quantify the endocytosis of soluble molecules (Johnson et al., 2007; Mangold et al., 2008; Turcotte et al., 2009; Chao et al., 2010; Chao and Raines, 2011), but not membrane-associated ones. Our expectation here was that upon endocytosis, the head group of lipid **1** would encounter endosomal esterases (Tian et al., 2012). The ensuing hydrolysis of the acetyl ester would unmask the rhodamine moiety and label the lumen with fluorescence

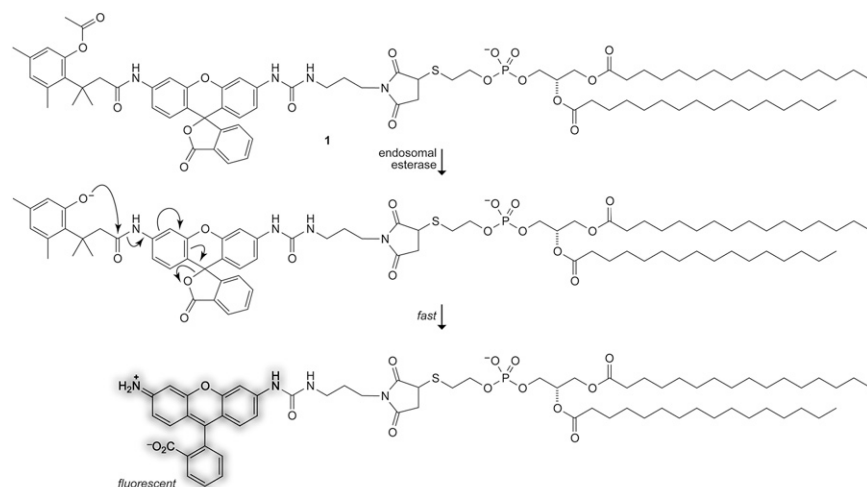


(Figure 1). The modularity of lipid **1** facilitated its synthesis by a route ending with the conjugate addition of 1,2-dihexadecanoyl-*sn*-glycero-3-phosphothioethanol to a trimethyl lock-rhodamine-maleimide fragment.

The phosphatidylglycerol moiety of lipid **1** is endogenous to humans and incorporates spontaneously into cellular membranes (Christie and Han, 2010). Most importantly for us, incorporated lipid **1** paints HeLa cells incubated at 37°C with a punctate staining pattern, as shown in Figure 2A. This pattern is indicative of vesicular localization and demonstrates that lipid **1** does indeed report on constitutive endocytosis. Notably, no fluorescence was observed in cells incubated at 4°C (Figure 2B), a temperature that does not allow for endocytosis (Tomoda et al., 1989).

Endocytic pathways are complex (Bissig et al., 2012). What then is the fate of lipid **1** after endocytosis? As shown in Figure 3A, we found that lipid **1** does not colocalize with fluorescently labeled transferrin, which is a marker of recycling endosomes (Ghosh et al., 1994). Consistent with this finding, lipid **1** that had been unmasked by a cellular esterase does not reappear on the plasma membrane (Figure 3B). These data indicate that lipid **1** does not recycle to the plasma membrane, but instead enters endosomes and traffics to other destinations. This attribute is desirable because fluorescence from lipid **1** reports only on new endocytic events (and not repetitious entry). As shown in Figure 3C, we found that lipid **1** does colocalize partially with LysoTracker red, a marker of late endosomes or lysosomes (Zhang et al., 1994), evincing its joining the canonical endosome-to-lysosome pathway along with trafficking to other subcellular compartments.

Lipid **1** can report on the rate of endocytosis. HeLa cells were labeled at 4°C with lipid **1** and then incubated for various times at 37°C. Fluorescence was quantified by flow cytometry. As shown in Figure 4, the mean fluorescence per cell increases over time until ~2 hr. This time course is consistent with morphological observations of mouse fibroblasts, which were seen engulfing their cell surface every 125 min (Steinman et al., 1976).

Finally, lipid **1** can reveal differences in endocytic rates between similar cells. HTB-125 and HTB-126 are noncancerous and cancerous breast cell lines that were derived from the same

Figure 1. Structure and Function of Lipid 1

Fluorescence is unmasked by an esterase encountered upon endocytosis.

patient (An et al., 2008). We used lipid **1** to assess endocytosis by cells in these matched lines, quantifying the results by flow cytometry. As shown in Figure 5, the increase in fluorescence over 3 hr of incubation at 37°C was 2.5-fold for HTB-125 cells. This increase was less than half that for HTB-126, which was 6.0-fold. Thus, in these cell lines, endocytosis is significantly more rapid in the cancerous than in the noncancerous cells. These differential rates could reflect more rapid turnover of cell-surface re-

ceptors in cancer cells (Mayor and Pagano, 2007), promoting a cancerous phenotype (Mosesson et al., 2008). We note that such an intrinsic difference in endocytic rate could provide an opportunity for therapeutic intervention by increasing the relative uptake of ptRNases or other macromolecular drugs (Sahay et al., 2010; Stephan and Irvine, 2011; Hymel and Peterson, 2012).

SIGNIFICANCE

We have designed and synthesized a head-group-modified lipid that can be incorporated into the plasma membrane, and that becomes fluorescent upon initiation of endocytosis. The lipid is trafficked to late endosomes and lysosomes and does not enter the recycling endosomal pathway. The increase in fluorescence can be monitored over time by flow cytometry and is utilized to reveal that cells from a breast cancer line undergo endocytosis more rapidly than do matched noncancerous cells. These data enable and encourage the use of lipid 1 in the exploration of endocytosis.

EXPERIMENTAL PROCEDURES

General

All reagents, unless noted, were from Aldrich Chemical (Milwaukee, WI) or Fisher Scientific (Hanover Park, IL), and were used without further purification. Thin-layer chromatography was performed by using aluminum-backed plates coated with silica gel containing F₂₅₄ phosphor and was visualized by UV illumination or developed with ceric ammonium molybdate stain. Flash chromatography was performed on open columns with silica gel-60 (230–400 mesh).

Nuclear magnetic resonance (NMR) spectra (see Supplemental Information) were obtained with a Bruker DMX-400 Avance spectrometer at the National Magnetic Resonance Facility at Madison. Mass spectrometry was performed with an Applied Biosystems MDS SCIEX 4800 matrix-assisted laser desorption/ionization (MALDI) time-of-flight mass spectrometer at the Mass Spectrometry Facility in the Biotechnology Center, University of Wisconsin-Madison.

The term “concentrated under reduced pressure” refers to the removal of solvents and other volatile materials using a rotary evaporator at water aspirator pressure (<20 mm Hg) while maintaining the water-bath temperature below 50°C. The term “high vacuum” refers to vacuum (<0.1 mm Hg) achieved by a mechanical belt-drive oil pump.

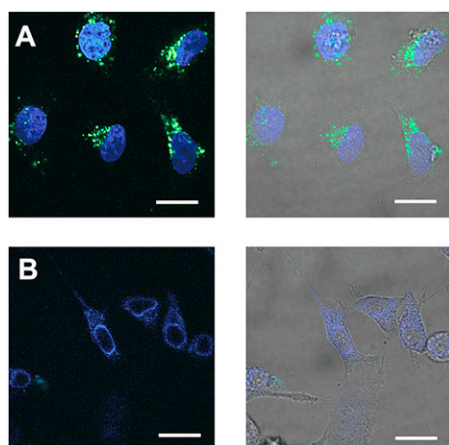


Figure 2. Lipid 1 Reports on Endocytosis

HeLa cells in serum-free Dulbecco's modified Eagle's medium (DMEM) were labeled for 3 hr at 4°C with lipid 1 (20 μM), washed with serum-free medium, and then incubated for 3 hr at (A) 37°C or (B) 4°C. Left: Confocal images. Right: Overlay of confocal and bright-field images. Blue dye, Hoechst 33342. Scale bars represent 20 μm.

Synthesis of Lipid 1

Maleimidourea-Rh₁₁₀ trimethyl lock (20 mg, 0.026 mmol) was synthesized as described previously (Lavis et al., 2006a) and dissolved in anhydrous chloroform (5 ml). The resulting solution was added to a flame-dried 10 ml round-bottom flask that had been flushed with Ar(g). Anhydrous triethylamine (20 μl, 0.14 mmol) was added, followed by 1,2-dihexadecanoyl-*sn*-glycero-3-phosphothioethanol, sodium salt (Avanti Polar Lipids, Alabaster, AL; 20 mg, 0.027 mmol). The flask was covered in foil, and the reaction mixture was stirred for 3 hr under Ar(g). Reaction progress was monitored by thin-layer chromatography (10% v/v methanol in dichloromethane [DCM]). Once the reaction was complete, the solvent was evaporated under reduced pressure and the residue was placed under high vacuum overnight. The crude product was purified by silica gel chromatography (10%–15% v/v methanol in DCM) to yield **1** as a white powder (26 mg, 66%). ¹H NMR (400 MHz, CDCl₃) δ: 8.52 (bs, 1H), 7.94 (d, *J* = 6.3 Hz, 1H), 7.79 (s, 1H), 7.64–7.50 (m, 2H), 7.39 (s, 2H), 7.05 (d, *J* = 6.9 Hz, 1H), 6.97 (bs, 1H), 6.76 (s, 1H), 6.64–6.56 (m, 2H), 6.51 (t, *J* = 7.2 Hz, 2H), 6.13 (s, 1H), 5.20 (s, 1H), 4.35 (d, *J* = 10.8 Hz, 1H), 4.15–3.86 (m, 6H), 3.52–3.40 (m, 2H), 3.24–2.92 (m, 7H), 2.87–2.75 (m, 1H), 2.63–2.57 (m, 2H), 2.41 (s, 3H), 2.34 (s, 3H), 2.28–2.15 (m, 7H), 1.64 (s, 6H), 1.56–1.46 (m, 4H), 1.33–1.14 (m, 48H), 0.87 (t, *J* = 6.2 Hz, 6H) ppm. ¹³C NMR (100 MHz, CDCl₃) δ: 178.5, 175.4, 174.0, 173.7, 172.1, 170.4, 170.0, 156.0, 153.0, 151.8, 151.7, 150.1, 142.5, 140.1, 139.0, 137.3, 135.4, 133.2, 133.1, 129.9, 128.3, 126.5, 125.0, 124.2, 123.5, 115.4, 114.7, 114.0, 111.6, 107.6, 106.0, 83.6, 70.6, 65.3, 63.9, 62.9, 50.9, 40.3, 39.6, 37.0, 36.5, 34.4, 34.2, 32.1, 30.2–29.2, 27.1, 26.7, 25.7, 25.1, 25.0, 22.8, 22.0, 20.3, 14.3 ppm. ³¹P NMR (162 MHz, CDCl₃) δ: –1.7 ppm. MS (MALDI): *m/z* 1487.75 [M+Na]⁺ ([C₈₀H₁₁₃O₁₇N₄NaPS]⁺ = 1,487.75).

Mammalian Cell Culture

HeLa, HTB-125, and HTB-126 cells were from the American Type Culture Collection (ATCC) (Manassas, VA). HeLa cells were grown in Dulbecco's modified Eagle's medium (DMEM) containing fetal bovine serum (FBS; 10% v/v), penicillin (100 U/ml), and streptomycin (100 μg/ml). HTB-125 cells were grown in Hybri-Care Medium supplemented with sodium bicarbonate (1.5 g/L), mouse epidermal growth factor (30 ng/ml), FBS (10% v/v), penicillin (100 U/ml), and streptomycin (100 μg/ml). HTB-126 cells were cultured in DMEM supplemented with bovine insulin (10 μg/ml), FBS (10% v/v), penicillin (100 U/ml), and streptomycin (100 μg/ml). Media and supplements were from Invitrogen (Carlsbad, CA), Sigma-Aldrich (Milwaukee, WI), or ATCC. Cells were cultured at 37°C in a humidified incubator containing CO₂ (g) (5% v/v).

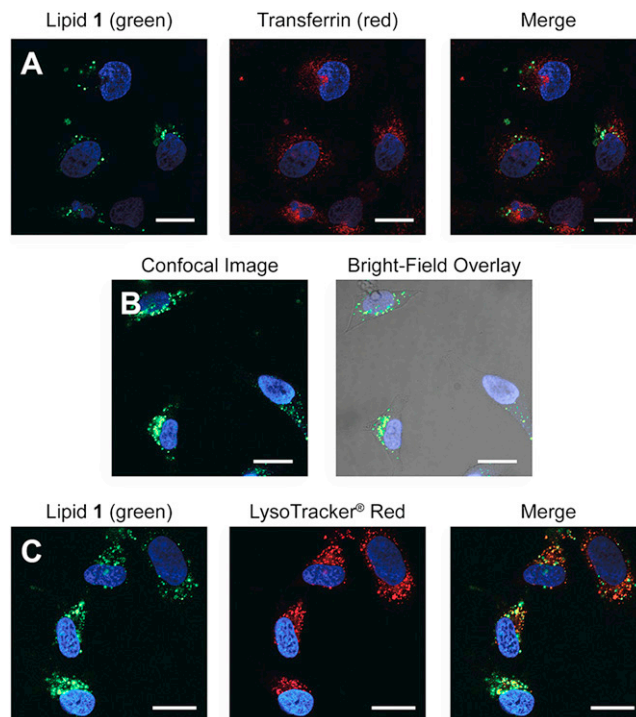


Figure 3. Lipid 1 Does Not Recycle to the Cell Surface

(A–C) HeLa cells in serum-free DMEM were labeled for 3 hr at 4°C with lipid 1 (20 μM), washed with serum-free medium, and then incubated for 3 hr at 37°C.

(A) Image after an Alexa Fluor 594 transferrin conjugate (1 μM) was added for the final 1 hr of a 3 hr incubation.

(B) Image after a 24 hr incubation.

(C) Image after LysoTracker red (50 nM) was added for the final 20 min of a 3 hr incubation.

Blue, Hoechst 33342. Scale bars represent 20 μm.

Microscopy

Imaging was performed with an Eclipse TE2000-U laser scanning confocal microscope from Nikon (Tokyo, Japan) equipped with an AxioCam digital camera from Carl Zeiss (Oberkochen, Germany). A blue-diode laser was used to provide excitation at 408 nm, and emission light was passed through a 35 nm band-pass filter centered at 450 nm. An argon-ion laser was used to provide excitation at 488 nm, and emission light was passed through a 40 nm band-pass filter centered at 515 nm. A HeNe laser was used to provide excitation at 543 nm, and emission light was passed through a 75 nm band-pass filter centered at 605 nm.

HeLa cells were plated 24 hr prior to experiments at a density of 1×10^5 cells in 1-cm-diameter glass-bottom dishes from Electron Microscopy Sciences (Hatfield, PA) in 1 ml of medium. On the day of an experiment, all cells, media, and pipette tips were precooled to 4°C for 2 hr. Next, cells were washed with serum-free DMEM (3 × 1 ml). Stock solutions of lipid 1 (50 mM in DMSO) were diluted to 10 mM with absolute ethanol. From this stock, 1 μl was added to 500 μl of serum-free DMEM, which was then vortexed vigorously and applied to the HeLa cells. Vehicle-treated cells were treated with 500 μl of serum-free DMEM containing 1 μl of ethanol. The labeling reaction was allowed to proceed for 3 hr at 4°C, after which the cells were washed with serum-free DMEM (3 × 1 ml). Cells were incubated for the given amount of time at 37°C. LysoTracker red (50 nM) from Invitrogen was used to stain acidic vesicles for the final 20 min of incubation at 37°C. Endocytic marker Alexa Fluor 594 transferrin (1 μM) from Invitrogen was used to stain recycling endosomes for the final 1 hr of incubation at 37°C. Nuclear counterstaining was performed with Hoechst 33342 (2 μg/ml) from Invitrogen for the final 5 min at 37°C. Cells were washed with serum-free DMEM prior to imaging.

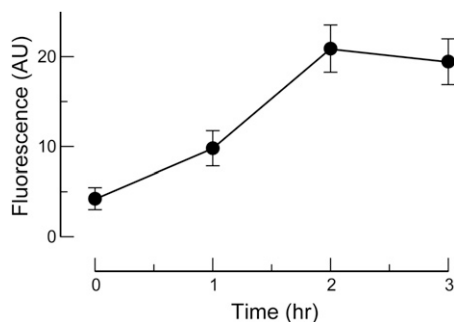


Figure 4. Time Course of Endocytosis by HeLa Cells

HeLa cells in serum-free DMEM were labeled for 3 hr at 4°C with lipid 1 (20 μM), washed with serum-free medium, and incubated for various times at 37°C. Fluorescence was quantified by flow cytometry. Values in arbitrary units (AU) are the mean ±SD from assays of 10,000 cells.

Flow Cytometry

Flow cytometry was performed at the University of Wisconsin Carbone Cancer Center with a FACSCalibur instrument equipped with a 488 argon-ion air-cooled laser from Becton Dickinson (Franklin Lakes, NJ). Fluorescence emission light was passed through a 30 nm band-pass filter centered at 530 nm. Cell lines were plated 24 hr prior to experiments at a density of 3×10^5 HeLa cells and 3.7×10^4 cells HTB-125 or HTB-126 cells in 6 ml of medium (vide supra) in T-25 tissue culture flasks from BD Biosciences (San Jose, CA). On the day of an experiment, all cells, media, and pipette tips were precooled to 4°C for 2 hr. Next, the cells were washed with serum-free DMEM (3 × 1 ml). Stock solutions of lipid 1 (50 mM in DMSO) were diluted with absolute ethanol to 10 mM. This stock solution in ethanol was added to serum-free DMEM to a final concentration of 20 μM and was mixed vigorously by vortexing. The medium was removed from the cells and was replaced with 1 ml of the labeling solution. Vehicle-treated cells were treated with 1 ml of serum-free DMEM containing 2 μl of ethanol. The labeling reaction was allowed to proceed for 3 hr at 4°C, after which the cells were washed with serum-free DMEM (3 × 1 ml). Cells were incubated for a known time at 37°C. Cells were then washed with Dulbecco's PBS (DPBS; 1 ml; Invitrogen) and treated with trypsin/EDTA (0.25% w/v; 750 μl) for 5 min at 37°C. The trypsin was neutralized with DMEM containing FBS (10% v/v; 750 μl), and the cells were collected by centrifugation (5 min at 400 × g). The supernatant was decanted, and the cell pellet was resuspended in 1 ml of DPBS. The cells were collected again by centrifugation (5 min at 400 × g). The supernatant was decanted, and the pellet was resuspended and fixed with 100 μl of aqueous formaldehyde (2% v/v) for 30 min in a vial covered with aluminum foil. This solution was diluted by adding DPBS to 1 ml, and the cells were collected by centrifugation (5 min at 400 × g). The supernatant was decanted, and the cell pellet was resuspended in 1 ml of DPBS. The suspension was strained through a 35 μm filter into a polystyrene flow cytometry test tube from BD Biosciences. The fixed cells were stored on ice until analyzed (~1–4 hr). The mean fluorescence per cell was determined in triplicate for 10,000 HeLa cells, 2,000 HTB-125 cells, and 2,000 HTB-126 cells, and the data were analyzed with FlowJo software from Tree Star (Ashland, OR).

SUPPLEMENTAL INFORMATION

Supplemental Information includes a ^1H , ^{13}C , and ^{31}P NMR spectrum of lipid 1 and can be found with this article online at <http://dx.doi.org/10.1016/j.chembiol.2013.03.016>.

ACKNOWLEDGMENTS

We are grateful to M. T. Walker for assistance in assay optimization and T. F. J. Martin for the use of his confocal microscope and contributive discussions. T.T.H. was supported by an advanced opportunity/graduate research scholar fellowship and molecular biosciences training grant T32 GM07215 from the

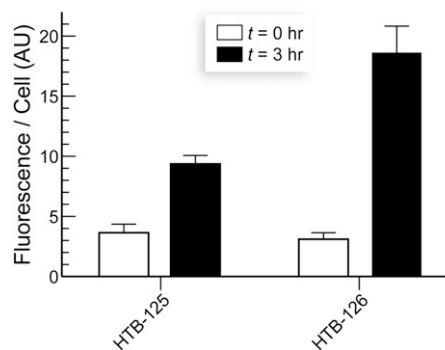


Figure 5. Rate of Endocytosis Is Greater in Cancerous Cells

Matched breast cell lines HTB-125 (noncancerous) and HTB-126 (cancerous) in serum-free DMEM were labeled for 3 hr at 4°C with lipid 1 (20 μM), washed with serum-free medium, and incubated for 0 or 3 hr at 37°C. Fluorescence was quantified by flow cytometry. Values are the mean ±SD from triplicate assays of 2,000 cells. HTB-125 cells: 3.7 ± 0.7 and 9.4 ± 0.7 AU; HTB-126: 3.1 ± 0.6 and 18.6 ± 2.2 AU.

National Institutes of Health (NIH). This work was supported by NIH grants R01 CA073808 and R01 GM044783 and made use of the National Magnetic Resonance Facility at Madison, which is supported by NIH grants P41 RR002301 and P41 GM066326, and the Mass Spectrometry Facility, which is supported by NIH grants P50 GM064598 and R33 DK007297 and National Science Foundation grants DBI-0520825 and DBI-9977525.

Received: December 4, 2012

Revised: February 24, 2013

Accepted: March 11, 2013

Published: April 18, 2013

REFERENCES

- An, S., Kumar, R., Sheets, E.D., and Benkovic, S.J. (2008). Reversible compartmentalization of *de novo* purine biosynthetic complexes in living cells. *Science* 320, 103–106.
- Arnold, U. (2008). Aspects of the cytotoxic action of ribonucleases. *Curr. Pharm. Biotechnol.* 9, 161–168.
- Bissig, C., Johnson, S., and Gruenberg, J. (2012). Studying lipids involved in the endosomal pathway. *Methods Cell Biol.* 108, 19–46.
- Chandran, S.S., Dickson, K.A., and Raines, R.T. (2005). Latent fluorophore based on the trimethyl lock. *J. Am. Chem. Soc.* 127, 1652–1653.
- Chao, T.-Y., and Raines, R.T. (2011). Mechanism of ribonuclease A endocytosis: analogies to cell-penetrating peptides. *Biochemistry* 50, 8374–8382.
- Chao, T.-Y., Lavis, L.D., and Raines, R.T. (2010). Cellular uptake of ribonuclease A relies on anionic glycans. *Biochemistry* 49, 10666–10673.
- Christie, W.W., and Han, X. (2010). *Lipid Analysis: Isolation, Separation, Identification and Lipidomic Analysis*, Fourth Edition (Cambridge, UK: Woodhead Publishing Limited).
- Cochilla, A.J., Angleson, J.K., and Betz, W.J. (1999). Monitoring secretory membrane with FM1-43 fluorescence. *Annu. Rev. Neurosci.* 22, 1–10.
- Conner, S.D., and Schmid, S.L. (2003). Regulated portals of entry into the cell. *Nature* 422, 37–44.
- Doherty, G.J., and McMahon, H.T. (2009). Mechanisms of endocytosis. *Annu. Rev. Biochem.* 78, 857–902.
- Fang, E.F., and Ng, T.B. (2011). Ribonucleases of different origins with a wide spectrum of medicinal applications. *Biochim. Biophys. Acta* 1815, 65–74.
- Ghosh, R.N., Gelman, D.L., and Maxfield, F.R. (1994). Quantification of low density lipoprotein and transferrin endocytic sorting HEp2 cells using confocal microscopy. *J. Cell Sci.* 107, 2177–2189.

- Gruenberg, J., and van der Goot, F.G. (2006). Mechanisms of pathogen entry through the endosomal compartments. *Nat. Rev. Mol. Cell Biol.* **7**, 495–504.
- Hanahan, D., and Weinberg, R.A. (2011). Hallmarks of cancer: the next generation. *Cell* **144**, 646–674.
- Hansen, C.G., and Nichols, B.J. (2009). Molecular mechanisms of clathrin-independent endocytosis. *J. Cell Sci.* **122**, 1713–1721.
- Hymel, D., and Peterson, B.R. (2012). Synthetic cell surface receptors for delivery of therapeutics and probes. *Adv. Drug Deliv. Rev.* **64**, 797–810.
- Ivanov, A.I., ed. (2007). *Exocytosis and Endocytosis* (Totowa, NJ: Humana Press).
- Johnson, R.J., Chao, T.-Y., Lavis, L.D., and Raines, R.T. (2007). Cytotoxic ribonucleases: the dichotomy of Coulombic forces. *Biochemistry* **46**, 10308–10316.
- Kerr, M.C., and Teasdale, R.D. (2009). Defining macropinocytosis. *Traffic* **10**, 364–371.
- Kok, J.W., ter Beest, M., Scherphof, G., and Hoekstra, D. (1990). A non-exchangeable fluorescent phospholipid analog as a membrane traffic marker of the endocytic pathway. *Eur. J. Cell Biol.* **53**, 173–184.
- Lavis, L.D., Chao, T.-Y., and Raines, R.T. (2006a). Fluorogenic label for biomolecular imaging. *ACS Chem. Biol.* **1**, 252–260.
- Lavis, L.D., Chao, T.-Y., and Raines, R.T. (2006b). Latent blue and red fluorophores based on the trimethyl lock. *ChemBioChem* **7**, 1151–1154.
- Lee, J.E., and Raines, R.T. (2008). Ribonucleases as novel chemotherapeutics: the ranpirinase example. *BioDrugs* **22**, 53–58.
- Levine, M.N., and Raines, R.T. (2012). Trimethyl lock: a trigger for molecular release in chemistry, biology, and pharmacology. *Chem. Sci.* **3**, 2412–2420.
- Levine, M.N., Lavis, L.D., and Raines, R.T. (2008). Trimethyl lock: a stable chromogenic substrate for esterases. *Molecules* **13**, 204–211.
- Lomax, J.E., Eller, C.H., and Raines, R.T. (2012). Rational design and evaluation of mammalian ribonuclease cytotoxins. *Methods Enzymol.* **502**, 273–290.
- Maier, O., Oberle, V., and Hoekstra, D. (2002). Fluorescent lipid probes: some properties and applications (a review). *Chem. Phys. Lipids* **116**, 3–18.
- Mangold, S.L., Carpenter, R.T., and Kiessling, L.L. (2008). Synthesis of fluorogenic polymers for visualizing cellular internalization. *Org. Lett.* **10**, 2997–3000.
- Mayor, S., and Pagano, R.E. (2007). Pathways of clathrin-independent endocytosis. *Nat. Rev. Mol. Cell Biol.* **8**, 603–612.
- McMahon, H.T., and Boucrot, E. (2011). Molecular mechanism and physiological functions of clathrin-mediated endocytosis. *Nat. Rev. Mol. Cell Biol.* **12**, 517–533.
- Mosesson, Y., Mills, G.B., and Yarden, Y. (2008). Derailed endocytosis: an emerging feature of cancer. *Nat. Rev. Cancer* **8**, 835–850.
- Rea, R., Li, J., Dharia, A., Levitan, E.S., Sterling, P., and Kramer, R.H. (2004). Streamlined synaptic vesicle cycle in cone photoreceptor terminals. *Neuron* **41**, 755–766.
- Richard, J.P., Melikov, K., Vives, E., Ramos, C., Verbeure, B., Gait, M.J., Chernomordik, L.V., and Lebleu, B. (2003). Cell-penetrating peptides. A reevaluation of the mechanism of cellular uptake. *J. Biol. Chem.* **278**, 585–590.
- Sahay, G., Alakhova, D.Y., and Kabanov, A.V. (2010). Endocytosis of nanomedicines. *J. Control. Release* **145**, 182–195.
- Steinman, R.M., and Cohn, Z.A. (1972). The interaction of soluble horseradish peroxidase with mouse peritoneal macrophages *in vitro*. *J. Cell Biol.* **55**, 186–204.
- Steinman, R.M., Brodie, S.E., and Cohn, Z.A. (1976). Membrane flow during pinocytosis. A stereologic analysis. *J. Cell Biol.* **68**, 665–687.
- Stephan, M.T., and Irvine, D.J. (2011). Enhancing cell therapies from the outside in: cell surface engineering using synthetic nanomaterials. *Nano Today* **6**, 309–325.
- Tian, L., Yang, Y., Wysocki, L.M., Arnold, A.C., Hu, A., Ravichandran, B., Sternson, S.M., Looger, L.L., and Lavis, L.D. (2012). Selective esterase-ester pair for targeting small molecules with cellular specificity. *Proc. Natl. Acad. Sci. USA* **109**, 4756–4761.
- Tomoda, H., Kishimoto, Y., and Lee, Y.C. (1989). Temperature effect on endocytosis and exocytosis by rabbit alveolar macrophages. *J. Biol. Chem.* **264**, 15445–15450.
- Turcotte, R.F., Lavis, L.D., and Raines, R.T. (2009). Onconase cytotoxicity relies on the distribution of its positive charge. *FEBS J.* **276**, 3846–3857.
- Zhang, Y.-Z., Diwu, Z., Mao, F., Leung, W., and Haugland, R.P. (1994). Novel fluorescent acidic organelle-selective dyes and mitochondrion-selective dyes that are well retained during cell fixation and permeabilization. *Mol. Biol. Cell* **5**(Suppl.), 113a.